Optical design and evaluation of Alvarez-type vision-training system

Wei Lou (娄 玮)[1], Dewen Cheng (程德文)[1,*], Luo Gu (顾 罗)[1], Weihong Hou (侯伟洪)[2], and Yongtian Wang (王涌天)[1]

[1]*School of Optics and Photonics, Beijing Institute of Technology, Beijing 100081, China*
[2]*Beijing NED+ Ltd., Beijing 100081, China*
**Corresponding author: cdwlxk@bit.edu.cn*

Received February 7, 2018; accepted May 8, 2018; posted online June 25, 2018

Myopia has become a noteworthy issue due to the increasing use of our eyes. We propose a continuous power variation vision-training device based on Alvarez lenses with the power ranging from −10 D to +2 D. First, we introduce the principle of Alvarez lenses and the evaluation method of dioptric power and astigmatism. Then, we optimize the optical system described by Zernike polynomials. Finally, we analyze the distributions of dioptric power and astigmatism with the overall surface analysis and fields of view (FOVs) analysis. The results show that the optical performance of an optimized system can meet the requirement within a 40° FOV.

OCIS codes: 220.3620, 220.1250, 330.7333, 330.7327.
doi: 10.3788/COL201816.072201.

With the development of display technology, portable electronic products with LCD/organic LED (OLED) screens are widely used, which leads to more eye diseases, especially myopia for the younger generation. Investigations show that 5% of Africans and 25% of Europeans and North Americans have suffered from mild to moderate myopia; what is worse, the percentage is pushed up to 80% for East Asians[1]. Especially, among Chinese aged over five, the proportion of myopia is 35.16%–39.21%[2]. The number of Chinese patients is the largest, and the incidence rate ranks the second in the world[3]. The deterioration of myopia may cause retinal detachment, amblyopia, incipient presbyopia, and many other visual diseases.

One of the major causes of acquired myopia is that staring at near objects for a long time will lead to visual fatigue. Myopia can be roughly categorized into refractive myopia and axial myopia[4]. Refractive myopia can be attributed to the increased curvature of refractive surfaces or the change in the refractive index of the eye. Axial myopia is because of the eye axis becoming elongated so that the object cannot be imaged exactly on the retina. Refractive myopia that is caused by the ciliary muscle over-contracting in the growing young generation, can be cured with the proper eye muscles treatments, while axial myopia is irreversible, as the eyeball structure has been changed.

According to the principle of optical imaging, the vision-training device, allowing the eye muscles to do regular adjustment exercises, can effectively improve the eyes' regulatory function. The device is relatively safe and effective in curing vision, which includes light glitter training, near–far training, and optical flipper plate training. Light glitter training is used to train the ciliary muscle by having the eyes track bright spots. But, it requires a high degree of cooperation without obvious effect[5]. The near–far training mainly focuses on a straight line, which is only helpful to improve center vision. In addition, most of such vision-training devices are bulky with complicated operation processes[6]. Optical flipper plate training switches dioptric power by manually flipping to carry out the eyes' adjustment exercises. However, the change of the power is abrupt in this method, so it is difficult for eyes to rapidly adjust[7]. Recently, the head-mounted vision-training device has been proposed to generate visual stimuli and improve the visual function of human eyes[8,9]. But, the users have a limited field of view (FOV) and cannot see the real scenario during the long training process, which will influence their normal activity and may even cause the problem of form deprivation.

For any effective vision-training program, good motivation and compliance is essential. With young children, this means that an adult must be available to ensure daily practice is maintained, for example, at least five times per week for the best success, for the duration of the vision-training program, which generally runs a course of between six weeks to four months, with 4 to 6 regular weekly in-office reviews[10]. However, this is possibly a problem for young children that have lots of study tasks, especially for Chinese children. As a result, the above training program might not be suitable. Even worse, they prefer to wear a pair of vision correction spectacles rather than curing their myopia. A vision-training program that will not affect their studies and normal life is very important for curing their vision and that is the goal of this Letter. We propose a novel training device based on Alvarez lenses. It looks like normal spectacles, and the dioptric power of the device can be changed smoothly and automatically by a micro actuator. Besides, the user can see the real scenario and do the training without any other manual manipulation. Young children can wear it for muscle training without interrupting their studies and normal life. So, in

this case, the vision-training program can be executed successfully.

Alvarez lenses are a zoom system that realizes variable dioptric power by relatively shifting double lenses. Earlier, Alvarez lenses were developed to solve the problem of the lack of accommodation in myopia[11]. The power variation of the system is linear with the lens translation. After movement, the Alvarez system is equivalent to a lens with specific dioptric power. Due to the development of freeform surface optimization[12–14] and manufacturing[15,16], some researches have developed Alvarez lenses. The original Alvarez lenses were only designed with a limited central FOV. In this Letter, the FOV of the system is optimized up to ±10°. Barbero *et al.*[17–19] indicated that dioptric power of the optimized Alvarez system varies smoothly, and astigmatism is uniform across the entire FOVs. Figure 1 illustrates the schematic diagram of Alvarez lenses.

The Alvarez optical system comprises two lenses that move with respect to each other along the x axis, and each lens is composed of a plane and a freeform surface. In order to decrease the total thickness of the system, two planes are facing inward with the freeform surfaces facing outward. In addition, the two lenses should be designed to be as close as possible, so that the system can be treated as a thin lens, which improves the imaging quality[20]. When moving to the configuration shown in Fig. 1(a), the system is equivalent to a convex lens, converging light beams, and helping relax the ciliary muscle to reduce the curvature of the eye lens. When moving to another configuration, as shown in Fig. 1(b), the system is equivalent to a concave lens, diverging light beams, and helping tense the ciliary muscle to expand the curvature of the eye lens. Figure 1(c) shows the initial configuration of the proposed system, and the two lenses can be designed with or without the initial dioptric power. All the movements can be driven by the micro-motors to easily control the dioptric power. At the same time, the vision treatment prescriptions data can be incorporated to make the vision training more scientific and effective.

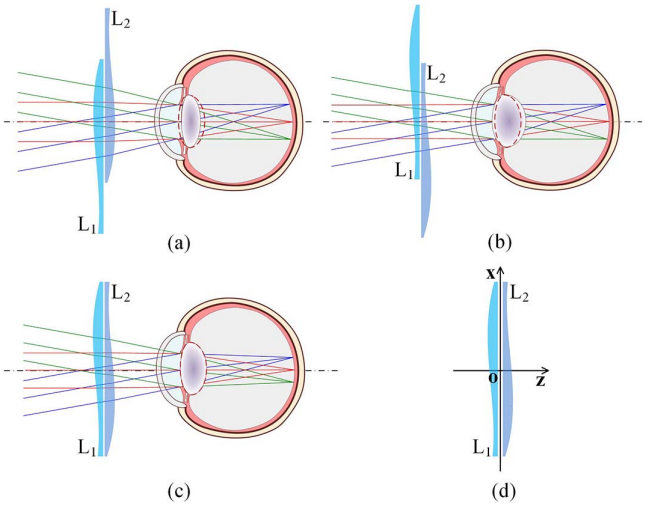

Fig. 1. Schematic diagram of Alvarez vision-training system with three different configurations.

The Alvarez system is defined in the Cartesian coordinate, whose origin is indicated by O in Fig. 1(d). Applying the thin lens approximation, the freeform surfaces corresponding to the two lenses L_1 (the front lens) and L_2 (the back lens) are described as[11]

$$\begin{cases} S_1(x,y) = a(xy^2 + x^3/3) + bx + t_0 \\ S_2(x,y) = -a(xy^2 + x^3/3) - bx + t_0 \end{cases}, \tag{1}$$

where the coefficient a reflects the ratio of dioptric power that varies with the movement. The coefficient b is the tilt coefficient that can be selected to reduce the lens thickness, and the constant t_0 is the central thickness added to the surface expression to maintain the feasible thickness.

When L_1 moves a distance Δd along the x axis, and L_2 moves the same distance Δd in the opposite direction, the thickness expressions will be written as

$$\begin{cases} S_1(x-\Delta d, y) = a(x-\Delta d)y^2 + 1/3a(x-\Delta d)^3 + b(x-\Delta d) + t_0 \\ S_2(x+\Delta d, y) = -a(x+\Delta d)y^2 - 1/3a(x+\Delta d)^3 - b(x+\Delta d) + t_0 \end{cases}. \tag{2}$$

Accumulating the expressions of L_1 and L_2, the description for the system can be calculated by

$$\begin{aligned} S_c &= S_1(x-\Delta d, y) + S_2(x+\Delta d, y) \\ &= -2a\Delta d(x^2+y^2) - 2/3a\Delta d^3 - 2b\Delta d + 2t_0. \end{aligned} \tag{3}$$

Dioptric power P is proportional to the second-order derivative of the surface expression[21]. In addition, the value is positive for convex surfaces and negative for concave surfaces. If the surface expression is represented as S, and the refractive index is denoted as n, we can derive P as

$$P = \frac{n-1}{2}\left(\frac{\partial^2 S}{\partial x^2} + \frac{\partial^2 S}{\partial y^2}\right). \tag{4}$$

From Eqs. (3) and (4), it can be obtained that the dioptric power of the Alvarez system has a linear relationship with $-4(n-1)a\Delta d$. The continuous power variation can be realized by changing the value of Δd linearly and smoothly.

Assuming that the maximum movement of the lens is ΔX, and the corresponding variation in dioptric power is ΔP, the coefficient a can be determined from Eq. (5):

$$a = \frac{\Delta P}{4(n-1)\Delta X}. \tag{5}$$

For ophthalmic systems, dioptric power is supposed to be accurate and uniform for a specified prescription; meanwhile, astigmatism is supposed to be as small as possible when the Alvarez system is in different configurations. Hence, we need to analyze the actual power and astigmatism distributions for the optimized system. In this Letter, dioptric power is described as the mean principal curvature of the surfaces multiplied by $(n-1)$. Astigmatism is described as the difference between the two principal curvatures of the surfaces multiplied by $(n-1)$.

The two principal curvatures of a point on the surface represent the maximum and minimum of the curvatures for this point, respectively, which are denoted as k_1 and k_2[22]. According to the definition, we develop the calculations for dioptric power P_i and astigmatism A_i at a certain point on the surface as

$$P_i = \frac{1}{2}(n-1)(k_1 + k_2), \tag{6}$$

$$A_i = (n-1)(k_1 - k_2), \tag{7}$$

where P_i and A_i are in m^{-1} denoted as D. We calculate distributions of dioptric power and astigmatism employing the above expressions to evaluate the optimized system.

The Zernike polynomials are selected to describe the freeform surfaces of the Alvarez system with c_n representing the coefficient of the nth term. As L_1 and L_2 have the same initial shape, the coefficients, except the constant term, in these two surface expressions are opposite to each other. After transforming the polar coordinate system into the Cartesian coordinate, the second, seventh, and eighth terms of the special surfaces (SPS) Zernike polynomials are employed to describe the surface in CODE V[23]:

$$\begin{aligned} S_1(x,y) &= c_2 x + c_7(x^3 - 3xy^2) + c_8(3x^3 + 3xy^2 - 2x) \\ &= (c_2 - 2c_8)x + (3c_8 + c_7)x^3 + (3c_8 - 3c_7)xy^2. \end{aligned} \tag{8}$$

Since the Zernike polynomials are defined on the unit circle, the coefficients need to be normalized[24]. Assuming that the surface is defined on a circle of radius R, the coefficients c_7 and c_8 can be calculated according to the corresponding relation between the coefficients of Eqs. (1) and (8) as the following:

$$c_7 = -c_8 = -\frac{\Delta P R^3}{24\Delta X(n-1)}. \tag{9}$$

Herein, two coefficients from Eq. (8), c_7 and c_8, can be solved when knowing the design requirements ΔX and ΔP with the specified refractive index n. The coefficient c_2 cannot be determined since it connects with x. However, it will not affect the dioptric power of the Alvarez system. Generally, the value of c_2 is decided to keep the lens thickness feasible.

Moreover, the resolution power of eyes is concentrated in the macular area with abundant visual cells[25], and the FOV for clear visual is about 5°[26]. So, we choose the range of −10°–10° to optimize the system, taking into account the eyes' rotation. The Alvarez system is positioned 12 mm in front of the stop, whose diameter is 6 mm, representing the eye pupil.

The lenses are rectangular with dimensions of $L \times H = 36\,\mathrm{mm} \times 30\,\mathrm{mm}$ and are made of polymethyl methacrylate (PMMA), whose refractive index n is about 1.49. The movement Δd ranges from −5 to 5 mm, while the corresponding power P varies from −10 D to 2 D, which means $\Delta X = 10\,\mathrm{mm}$, and $\Delta P = -12$ D. Optimization variables are composed of the Zernike coefficients numbered from 1 to 21 and the radius of the sphere basis. During the optimization process, the coefficients of L_1 and L_2 can vary randomly, in that L_1 and L_2 are not required to have the exact same surface profile. Before optimization, the normalized radius R, the radius of curvature r, and the Zernike coefficients c_i for L_1 and L_2 are shown in Table 1.

Based on the initial parameters, we can depict the distributions of dioptric power and astigmatism for L_1, as shown in Fig. 2. The dioptric power contours are a set of parallel lines perpendicular to the x axis and decrease with x linearly, which is opposite of L_2. The astigmatism contours are a set of parallel lines perpendicular to the y axis and are symmetric about the x axis. In the thin lens approximation, dioptric power of the two lenses is superimposed, and astigmatism is compensated to zero for the vision-training system.

Table 1. Initial System Parameters

Parameter	L_1	L_2
R (mm)	25	25
r (mm)	−250	250
c_2	1.0000	1.0000
c_7	1.5625	1.5625
c_8	−1.5625	−1.5625

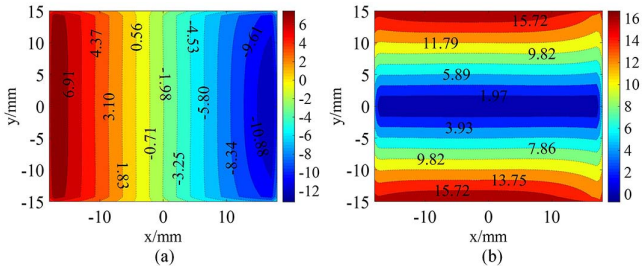

Fig. 2. Distributions of (a) dioptric power and (b) astigmatism for one lens of the Alvarez system.

Astigmatism is the main aberration for the Alvarez system due to the small pupil of human eyes. During the optimization process, the two lenses approach the condition of thin lenses, which may cause interlacement at the edge of the lens. Since the edge of the spectacles would not be used, the shape of the lens can be changed into an ellipse. After optimization, the normalized radius R, the radius of curvature r, and the Zernike coefficients c_i for L_1 and L_2 are shown in Table 2.

Figure 3 shows the distributions of dioptric power and astigmatism for the optimized system. The movement of lenses will reduce the effective length of the vision-training system, and the maximum movement of 5 mm leads to the minimum overlap length of 26 mm. We set an effective ellipse area with the horizontal length of 24 mm and vertical length of 16 mm circled by the red curve, where the areas of interest for dioptric power and astigmatism are located. It can be observed from these figures that in the ellipse area, dioptric power is uniform for different values of Δd and is close to the theoretical value P. Astigmatism is small with a simultaneously homogeneous distribution. Nevertheless, the dioptric power is quite different from the theoretical value, and astigmatism increases rapidly in the invalid edge region.

Table 2. Optimized System Parameters

Parameter	L_1	L_2
R (mm)	25	25
r (mm)	−173.6265	173.6416
c_1	0.3534	−1.045
c_2	−2.5000	−2.5000
c_3	−2.2894	−2.4998
c_4	0.4354	0.8663
c_5	−0.0585	−0.6200
c_6	−0.0214	0.0008
c_7	1.3823	1.0992
c_8	−1.4839	−1.4639
c_9	−1.7909	−1.9615
c_{10}	1.7165	1.9533
c_{11}	−0.0765	−0.3459
c_{12}	0.1535	0.2997
c_{13}	−0.1117	−0.1221
c_{14}	−0.0043	0.0035
c_{15}	0.0090	−0.0023
c_{16}	0.1342	0.2628
c_{17}	−0.0454	−0.1387
c_{18}	0.0269	0.0430
c_{19}	−0.4926	−0.5321
c_{20}	0.4681	0.5334
c_{21}	−0.4379	−0.5455

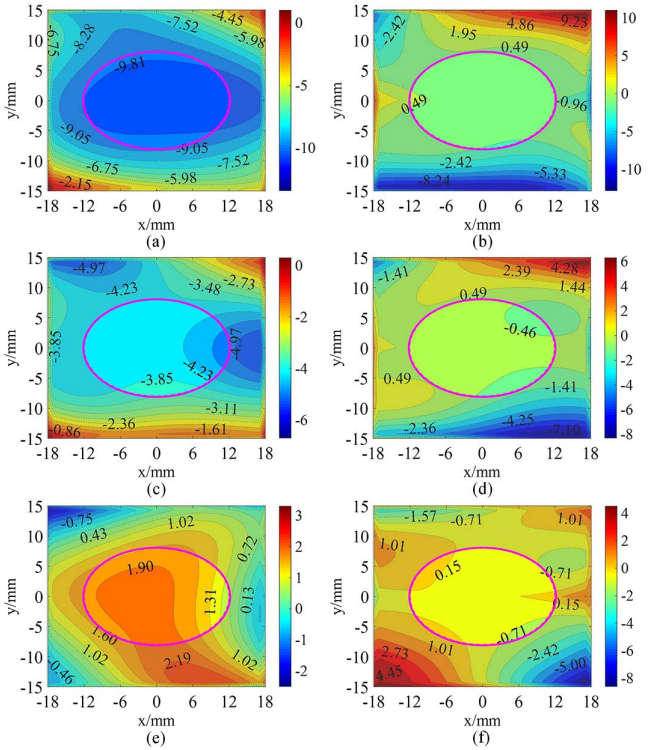

Fig. 3. Distributions of dioptric power (left) and astigmatism (right) of the optimized Alvarez system. In (a) and (b), $\Delta d = -5$ mm, $P = -10$ D. In (c) and (d), $\Delta d = 0$ mm, $P = -4$ D. In (e) and (f), $\Delta d = 5$ mm, $P = 2$ D.

From the above analysis, we could acquire whether the design fulfills the need of power variation or not. The light from the FOVs beyond the central one is not perpendicular to the surface of the lens but inclines to the tangent plane of the lens, as illustrated in Fig. 4. As a result, the compensation between the two lenses is not simply perpendicular to each other. The values of dioptric power calculated by the accumulation of L_1 and L_2 are not accurate enough, so we need to analyze the dioptric power across the FOVs.

We first calculate the intersections of the light from the FOVs and the surfaces and, then, add the dioptric power of L_1 and L_2 at that point to obtain the power distributions across the FOVs. The same method is applied to

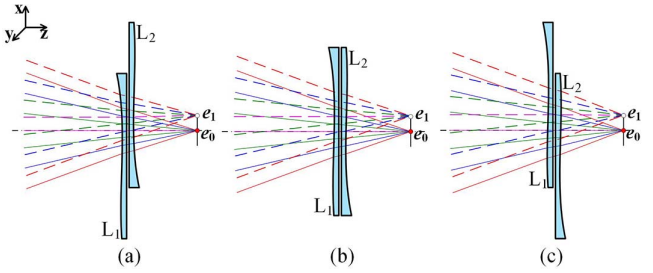

Fig. 4. Schematic diagram of the light from FOVs intersecting the surfaces with three configurations.

the analysis of astigmatism. In order to explore the influence of the evaluation point coordinates, we analyze the distributions at two points of the exit pupil plane. We denote the actual dioptric power and astigmatism at evaluation point e by $P_s(\text{fov}, e)$ and $A_s(\text{fov}, e)$, respectively, where fov ranges from $-20°$ to $20°$, representing the FOVs, and e can be e_0 and e_1, representing the center (0, 0) and the edge (3, 0) of the exit pupil plane.

Figure 5 visualizes the distributions of dioptric power and astigmatism across the entire FOVs located at the exit pupil center e_0 before optimization. Figures 5(a), 5(c), and 5(e) show the power distributions and Figs. 5(b), 5(d), and 5(f) show the astigmatism distributions. Here, $P = -10$ D in Figs. 5(a) and 5(b); $P = -4$ D in Figs. 5(c) and 5(d); $P = 2$ D in Figs. 5(e) and 5(f). The x direction and the y direction FOVs are represented by α and β in degree (°), ranging from $-20°$ to $20°$. Shown in Fig. 5, the dioptric power is a little far from the theoretical values with choppy distributions. The values of astigmatism are large at the edge. After optimization, the differences have been reduced.

Figure 6 visualizes the distributions of dioptric power across the entire FOVs located at the exit pupil after optimization. The theoretical value of dioptric power P is -10 D in Figs. 6(a) and 6(b), and the maximum deviation

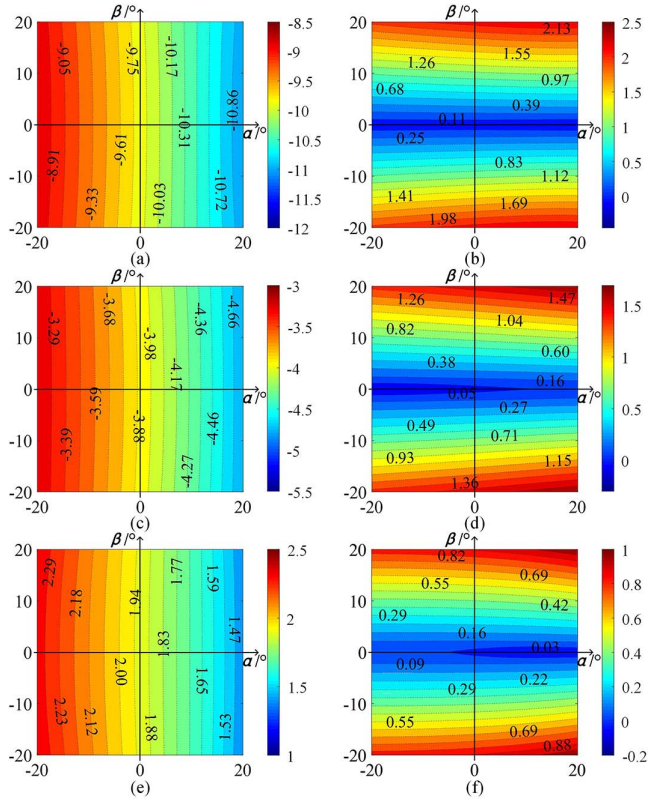

Fig. 5. Distributions of dioptric power (left) and astigmatism (right) across FOVs of the initial Alvarez system at the evaluation point $(0, 0)$. The distributions are based on (a) $P_s(\text{fov}, e_0)$ and (b) $A_s(\text{fov}, e_0)$, where $P = -10$ D; (c) $P_s(\text{fov}, e_0)$ and (d) $A_s(\text{fov}, e_0)$, where $P = -4$ D; (e) $P_s(\text{fov}, e_0)$ and (f) $A_s(\text{fov}, e_0)$, where $P = 2$ D, respectively.

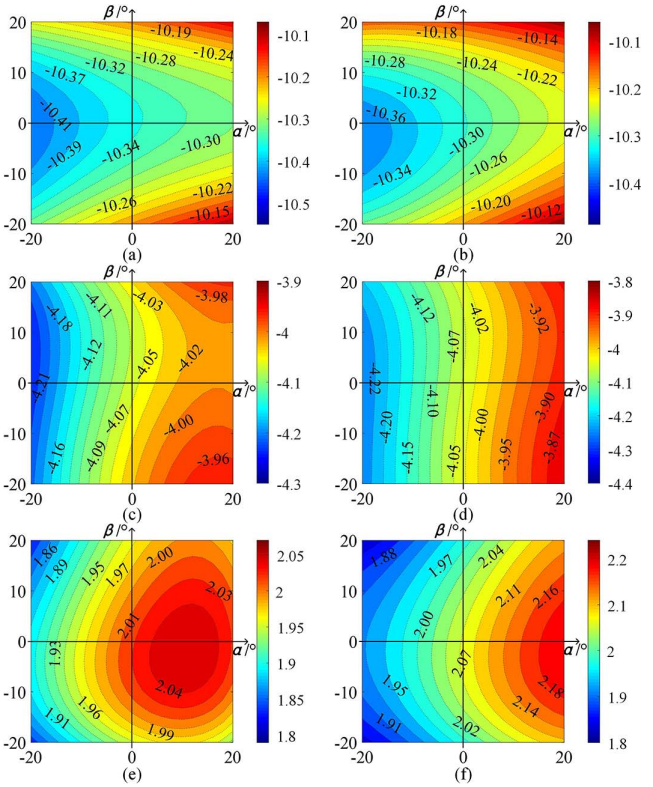

Fig. 6. Dioptric power distributions across FOVs of the optimized Alvarez system at the evaluation points (0, 0) (left) and (3, 0) (right). The distributions are based on (a) $P_s(\text{fov}, e_0)$ and (b) $P_s(\text{fov}, e_1)$, where $P = -10$ D; (c) $P_s(\text{fov}, e_0)$ and (d) $P_s(\text{fov}, e_1)$, where $P = -4$ D; (e) $P_s(\text{fov}, e_0)$ and (f) $P_s(\text{fov}, e_1)$, where $P = 2$ D, respectively.

of power is about 0.4 D. The theoretical value of dioptric power P is -4 D in Figs. 6(c) and 6(d), and the maximum deviation of power is about 0.3 D. The theoretical value of dioptric power P is 2 D in Figs. 6(e) and 6(f), and the maximum deviation of power is about 0.2 D. According to the analysis of power distributions across FOVs, the values of dioptric power are basically consistent with the theoretical values, and the variation is within an acceptable range. In addition, as seen from the comparison of Figs. 6(a), 6(c), 6(e) and Figs. 6(b), 6(d), 6(f), the movement of the evaluation point will cause the center of power distributions to move along the corresponding direction.

Figure 7 visualizes the distributions of astigmatism across the entire FOVs located at the exit pupil after optimization corresponding to Fig. 6. According to the distributions, we can see that the astigmatism values are close to zero, especially for the central FOV, and vary smoothly. The whole distributions are symmetric about the α axis. Compared with the astigmatism at the evaluation point (0, 0), the absolute values of the astigmatism at the point (3, 0) increase by about 0.1 D. In addition, the effect of the evaluation point change is more obvious in Figs. 7(b) and 7(d). In conclusion, the movement of the evaluation point will change values of dioptric power and astigmatism a little bit but not obviously. Moreover,

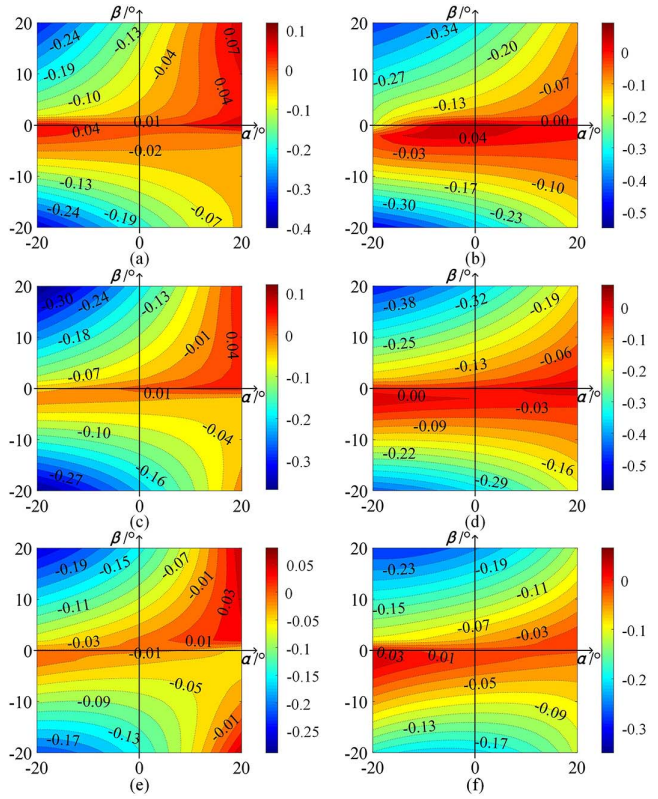

Fig. 7. Astigmatism distributions across FOVs of the optimized Alvarez system at the evaluation points $(0, 0)$ (left) and $(3, 0)$ (right). The distributions are based on (a) $A_s(\text{fov}, e_0)$ and (b) $A_s(\text{fov}, e_1)$, where $P = -10$ D; (c) A_s (fov, e_0) and (d) $A_s(\text{fov}, e_1)$, where $P = -4$ D; (e) $A_s(\text{fov}, e_0)$ and (f) $A_s(\text{fov}, e_1)$, where $P = 2$ D, respectively.

when the evaluation coordinates are $(-3, 0)$, $(0, 3)$, and $(0, -3)$, we can obtain the same analysis results.

After optimization, dioptric power and astigmatism of the Alvarez system described by the Zernike polynomials are uniform. For different power configurations, the optical performance of the final system is good enough to meet the requirements of vision training in the $-20°$ to $20°$ FOV using the overall surface analysis and FOVs analysis. Future work would concern the fabrication of the optimized Alvarez system, which would use the injection-molding method. As we utilize higher-order Zernike polynomials, particular attention should be paid to the change of the coefficients and the slopes of the surfaces. After simulation and calculation, when the surface deviation is in the range of 10 μm, the change in dioptric power is less than 0.4 D, and the change in astigmatism is less than 0.1 D.

The Alvarez system with two thin freeform lenses can be used as a portable vision-training device, joining control equipment, to help ciliary muscle exercise. Shifting the two lenses of the system in opposite directions will realize linear variation in dioptric power with the continuous variation range −10 D to +2 D. The device is lightweight and so convenient that it will compensate the defects of the common training device, including bulky shape, complicated training modes, and form deprivation. It can carry out vision training most of the time and places without influencing daily activities, which may be particularly helpful to vision therapy for young children who are on the journey of the academic road.

This work was supported by the National Key Research and Development Program of China (No. 2016YFB1001502) and the National Natural Science Foundation of China (No. 61727808). We thank Synopsys for providing the educational license of CODE V.

References

1. J. S. Rahi, P. M. Cumberland, and C. S. Peckham, Ophthalmology **118**, 797 (2011).
2. L. Li, *Report on National Vision Care in China* (Peking University, 2016).
3. J. Wallman and J. Winawer, Neuron **43**, 447 (2004).
4. J. R. Cooling, *Dictionary of Visual Science* (Butterworth-Heinemann, 1997).
5. J. H. Shao, Chin. Med. Eng. **24**, 113 (2016).
6. D. P. Hu and J. C. Sun, Chin. J. Rehabil. **26**, 149 (2011).
7. J. Xu, Chin. Glass Sci. Technol. **05**, 127 (2013).
8. Q. L. Deng, B. S. Lin, H. T. Chang, G. S. Huang, and C. Y. Chen, J. Disp. Technol. **10**, 433 (2014).
9. D. Todd and B. Sabel, "Method and device for delivering visual stimuli with head mounted display during vision training," U.S. Patent 0,038,142 A1 (February 15, 2007).
10. Strachan Eyecare Plus, "Vision therapy," http://www.str-achaneyecare.com.au (2013).
11. L. W. Alvarez, "Two-element variable-power spherical lens," U.S. Patent 3,305,294 (February 21, 1967).
12. D. Cheng, Q. Wang, Y. Wang, and G. Jin, Chin. Opt. Lett. **11**, 031201 (2013).
13. T. Yang, J. Zhu, and G. Jin, Chin. Opt. Lett. **14**, 060801 (2016).
14. T. Yang, G. Jin, and J. Zhu, Chin. Opt. Lett. **10**, 060202 (2017).
15. M. Kong, Z. Gao, X. Li, S. Ding, X. Qu, and M. Yu, Opt. Express **17**, 13283 (2009).
16. D. Cheng, H. Hua, M. M. Talha, and Y. Wang, Appl. Opt. **48**, 2655 (2009).
17. S. Barbero, Opt. Express **17**, 9376 (2009).
18. S. Barbero and J. Rubinstein, J. Opt. **13**, 125705 (2011).
19. M. Peloux and L. Berthelot, Appl. Opt. **53**, 6670 (2014).
20. T. J. Suleski and M. A. Davies, Opt. Eng. **51**, 3006 (2012).
21. R. Blendowske, E. A. Villegas, and P. Artal, Optom. Vis. Sci. **83**, 666 (2006).
22. J. Oprea, *Differential Geometry and Its Applications* (Elsevier Science, 1991).
23. Synopsys, *CODE V Reference Manual* (2017).
24. R. J. Noll, J. Opt. Soc. Am. **66**, 207 (1976).
25. H. Gross, *Handbook of Optical Systems* (Wiley-VCH, 2005).
26. M. M. Kong and Z. Li, Chin. Opt. Lett. **12**, 113301 (2014).